ERRATUM

SLAC-PUB-634, ITP-336, CPT-10

S. J. Brodsky, A. C. Hearn, and R. G. Parsons

DETERMINATION OF THE REAL PART OF THE COMPTON AMPLITUDE AT A NUCLEON RESONANCE

Reference 10 should be R. A. Berg and C. N. Lindner, Nuclear Physics 26, 259 (1961).

The result for X_1 given in Eq. (15) and the scale for ϵ in figures 2 and 3 should be reduced by a factor of 4.

We wish to thank Dr. R. Simonds for helpful correspondence.

SLAC-PUB-634
ITP-336
CPT-10
July 1969
(TH) and (EXP)

DETERMINATION OF THE REAL PART OF THE COMPTON AMPLITUDE AT A NUCLEON RESONANCE*

Stanley J. Brodsky

Stanford Linear Accelerator Center
Stanford University, Stanford, California 94305

and

Anthony C. Hearn†

Institute of Theoretical Physics
Department of Physics, Stanford University, Stanford, California 94305

and

Ronald G. Parsons

Center for Particle Theory
Department of Physics, The University of Texas, Austin, Texas 78712

(Submitted to Phys. Rev.)

---

* Supported in part by the U. S. Atomic Energy Commission, the National Science Foundation, and the Air Force Office of Scientific Research, Office of Aerospace Research, U. S. Air Force, under AF OSR Contract Nr. F44620-68-C-0075. Computer time supported in part by the Stanford Artificial Intelligence Project through the Advanced Research Project Agency of the Office of the Secretary of Defense (SD-183).

† Present Address: Physics Department, University of Utah, Salt Lake City, Utah 84112.

ABSTRACT

The real part of the virtual Compton amplitude can be directly determined from measurements of electron (or muon) bremsstrahlung or pair photoproduction. In general, the interference of the Compton amplitude with the Bethe-Heitler amplitude for pair production or bremsstrahlung yields a contribution to the cross section which is antisymmetric when the leptons are interchanged. This interference contribution thus produces different cross sections for electron and positron bremsstrahlung at a given scattering energy and angle. Also the counting rate for pair production will depend on which lepton has the greater momentum. The determination of the real part of the Compton amplitude would supply information on the isobar resonance shape, test the dispersion relation for the forward amplitude, and resolve uncertainties in the determination of the nucleon resonances. A simple estimate for the lepton asymmetry of the pair production cross sections due to the forward Compton amplitude is given in addition to a complete calculation of the effect of the first nucleon resonance using the isobar model. The results are also discussed for nuclear targets. For the latter case, a broadening of the isobar decay width due to absorption in the nuclear medium must be taken into account.

I. INTRODUCTION

A direct measurement of the real part of the proton Compton scattering amplitude could be of considerable theoretical interest. In addition to resolving uncertainties in the determination of nucleon resonances[1], the determination of the real part of the Compton amplitude could supply important information on the resonant shape of a hadronic amplitude. Further, if the real part could be determined for forward Compton scattering, a test of the Kramers-Kronig relation is possible:

$$A(\omega, 0^{o}) = -\frac{\alpha}{M_p} + \frac{i\omega}{4\pi}\,\sigma_{tot}(\omega) + \frac{\omega^2}{2\pi^2}\,P\int_0^\infty d\omega'\,\frac{\sigma_{tot}(\omega')}{\omega'^2-\omega^2}\ . \qquad (1)$$

The real part of the amplitude is given to order α by the Thomson limit at threshold plus a dispersion integral over the total hadronic photon-absorption cross section. Other theoretical applications of the real Compton amplitude will be discussed in later sections.

In this paper we wish to emphasize that the real part of the virtual Compton amplitude (with one photon off its mass shell) can be directly determined from measurements of electron (or muon) bremsstrahlung or pair production. The contributing diagrams are shown in Fig. 1.

In general the interference of the virtual Compton amplitude (which is odd under lepton charge conjugation) with the first Born approximation Bethe-Heitler amplitudes (which are even under lepton charge conjugation) yields a contribution to the cross section which is antisymmetric under the interchange of the leptons. This interference contribution produces, for example, different cross sections for electron and positron bremsstrahlung

at a given scattering energy and angle. Similarly, in asymmetric coincidence pair production measurements, the production rate will depend on which lepton has the greater momentum. The quantity

$$\epsilon(\delta) = \frac{N_+(\delta) - N_-(\delta)}{N_+(\delta) + N_-(\delta)} = \frac{d\sigma_{int}(\delta)}{d\sigma_{BH}(\delta) + d\sigma_{Comp}(\delta)} , \qquad (2)$$

where $N_-(\delta)$ $[N_+(\delta)]$ is the production rate when the electron and positron are detected mirror symmetrically in angle but the electron [positron] has δ less momentum than the other lepton, is directly proportional to the real part of the Compton amplitude.

In addition to the Compton contribution, second and higher order Born amplitudes can contribute to the charge asymmetry; complete calculations have been given in Ref. (2). For the experiments discussed in this paper using hydrogen and carbon targets, this contribution is, however, less than 1% and will be neglected. Similarly, we expect the interference of the higher Born amplitudes with the Compton amplitude to be small. The radiative corrections can be another source of asymmetry but this contribution involves photon emission from the nucleus and is therefore negligible.

Asymmetric bremsstrahlung and pair production experiments thus make possible a direct determination of the real part of the virtual Compton amplitude via interference with a known real electrodynamic amplitude. The validity of the Bethe-Heitler amplitudes as given by quantum electrodynamics has been established for (e^+, e^-), (μ^+, μ^-), and (e^-, γ) invariant pair mass up to 1 BeV.[3]

Recently, Asbury et al.[4] measured large-angle asymmetrical e^+e^- pair production on carbon in the invariant pair mass region 770 ± 50 MeV/c^2 (the region of the ρ^o) as a means of determining the phase and magnitude of the virtual Compton amplitude at relatively high photon energy (2.8 to 4.5 GeV). The results are consistent with an imaginary production amplitude for the photoproduction of ρ^o on carbon.

In this paper we emphasize the utility of lepton asymmetry in bremsstrahlung and pair production for the study of the real part of the virtual Compton amplitude in the region of the low-lying nucleon resonances[5]. The resonance signal takes the form of a principal value part of a Breit-Wigner pole shaped by known kinematic factors. Measurements of the Compton amplitude will make possible a detailed study of the resonance shape and are particularly sensitive to the energy dependence of the width parameter in the resonant amplitude. As the photon energy is increased, higher I = 1/2 and I = 3/2 nucleon resonances can be explored. A sensitive experiment would produce information on coupling constants, masses, and widths of the s-channel excitations.

By measuring the virtual Compton amplitude, additional information on the dependence on virtual invariant photon mass can be obtained. In the isobar model for the Compton amplitude near a nucleon resonance, the γNN^* form factor can be obtained for space-like and time-like virtual photon momentum from the bremsstrahlung and pair production experiments respectively. The γNN^* form factor results in the space-like region would be complimentary to those obtained from inelastic electron scattering[6]. An extrapolation to real photon forward Compton scattering is of course required to test Eq. (1).

In the next section a simple approximate formula is discussed which gives the correct qualitative features of the Compton contribution to pair production. In Section III we write the Compton amplitude in terms of a simple isobar model consistent with that used recently by Dufner and Tsai[6] in their comprehensive analysis of N^*_{33} parameters. Quantitative predictions are presented. Finally, in Section IV we extend the analysis of the Compton contribution in pair production to the case of nuclear targets.

II. ESTIMATE OF THE COMPTON CONTRIBUTION

We will denote the amplitudes associated with the Feynman diagrams in Fig. (1) by

B_1 = Bethe-Heitler amplitude in first Born approximation (Figs. 1a and 1b)

B_2 = Bethe-Heitler amplitude in second Born approximation (Figs. 1c, 1d, and 1e)

C = Born approximation proton Compton amplitude (Fig. 1f)

C^* = Compton amplitude in the isobar model near the first nucleon resonance ($s \sim M^{*2}$).

The contributions of $B_1 \times B_1$, $B_1 \times C$, and $C \times C$ have been given by Bjorken, Drell, and Frautschi[7] for pair production and bremsstrahlung. The contribution of $B_1 \times B_2$ is given in Ref. 2.

It will be useful to review the contribution of the nucleon pole contribution to electron pair production. To leading order in M^{-1}, the result of Ref. 7 is

$$\frac{d\sigma_{int}(B_1 \times C)}{d\sigma(B_1 \times B_1) + d\sigma(C \times C)} \cong \frac{\lambda_{12}}{\lambda_{11}} \tag{3}$$

where

$$\lambda_{11} = 4m_e^2 \overline{\sum_{\substack{\text{spin,}\\ \text{pol}}}} M_{B_1}^{\dagger} \cdot M_{B_1}$$

$$= \frac{2}{q^4}\left[\frac{m_e^2 q^2}{2(k\cdot p_1)^2} + \frac{m_e^2 q^2}{2(k\cdot p_2)^2} - \frac{k\cdot p_+}{k\cdot p_-} - \frac{k\cdot p_-}{k\cdot p_+} - \frac{q^2(p_+\cdot p_- + E_+^2 + E_-^2)}{k\cdot p_+ k\cdot p_-}\right] \tag{4}$$

and

$$\lambda_{12} = 4m_e^2 \overline{\sum_{\substack{\text{spin,}\\ \text{pol}}}}\left[M_{B_1}^{\dagger} M_C + M_C^{\dagger} M_{B_1}\right]$$

$$= \frac{-4}{M}\frac{1}{q^2}\frac{1}{(p_+ + p_-)^2}\left[\frac{(E_+ + E_-)p_-\cdot p_+ + E_- k\cdot p_+ - E_+ k\cdot p_-}{k\cdot p_+}\right. \tag{5}$$

$$\left. - \frac{(E_+ + E_-)p_-\cdot p_+ + E_+ k\cdot p_- - E_- k\cdot p_+}{k\cdot p_-}\right] + \tilde{\lambda}_{12}\,.$$

We have taken the proton as a static charge distribution and $F_1(q^2) \sim 1$. The only m_e^2 terms which are kept are those which can give important contributions when the cross section is integrated over lepton angles. The interference contribution $\tilde{\lambda}_{12}$ is at least of third order in the lepton-positron asymmetry parameters and will not be required for our purposes.

Let us, for simplicity, consider a specific case of asymmetric electron pair production in which the leptons are detected mirror symmetrically to the incident beam ($\theta_+ = \theta_- = \theta$, $\phi_+ - \phi_- = \pi$) but the electron has δ more energy than the positron ($\delta = E_- - E_+$). We then obtain the simple result

$$\epsilon = \frac{\delta}{M}\,\theta^2\left[1 + 0(\theta^2) + 0\left(\frac{\delta^2}{E_\pm^2}\right) + 0\left(\frac{E_\pm^2}{M^2}\right)\right] \tag{6}$$

where ϵ is the asymmetric quantity defined in Eq. (2). Thus, for typical cases ($\delta \sim 200$ MeV, $\theta \sim 20^{\circ}$) the nucleon pole contribution to ϵ is of order 2%. This result would be essentially unchanged for a nuclear target. (See Section IV).

One can easily show that the leading contribution to ϵ arises from the real photon forward Compton scattering amplitude; that is, the $\bar{u}(p')\,\epsilon\cdot\epsilon'\,u(p)$ part of the nucleon Born terms. The remainder of the nucleon Born amplitude contributes terms of order δ^3 to ϵ_p (the $\tilde{\lambda}_{12}$ term). The leading result is also unchanged if instead of $\epsilon\cdot\epsilon'$ we use a gauge-invariant form for the virtual amplitude such as

$$\epsilon\cdot\epsilon' - \frac{\epsilon\cdot k'\,\epsilon\cdot k}{k\cdot k'} \quad .$$

Thus to leading order in δ, we expect the forward real Compton amplitude to dominate and

$$\epsilon \cong \frac{\delta}{M}\,\theta^2\left[-\frac{M_p}{\alpha}\,\mathrm{Re}\,A(\omega,0^{\circ})\right] \tag{7}$$

where $A(\omega,0^{\circ})$ is defined as in Eq. (1).

We can get a rough estimate of the contribution of excited nucleon states by approximating

$$A(\omega,0^{\circ}) = \frac{-\alpha}{M} + \frac{i\omega^*\sigma_{tot}(\omega^*)}{4\pi}\left[\frac{i\Gamma/2}{\omega-\omega^*+i\Gamma/2}\right] \tag{8}$$

for $\omega \sim \omega^*$. Then

$$\epsilon \cong \frac{\delta}{M}\,\theta^2\left[1+\frac{M_p}{\alpha}\,\frac{(\omega-\omega^*)\frac{\Gamma}{2}\,\omega^*\sigma_{tot}(\omega^*)}{4\pi[(\omega-\omega^*)^2+(\Gamma/2)^2]}\right] \tag{9}$$

The absorption cross section at the first resonance N^*_{33} is approximately 550 μb,[8] leading to an asymmetry approximately 4 times the Born contribution for $\omega = \omega^* + \Gamma/2$. Since each nucleon contributes equally for an I = 3/2 resonance, the asymmetry for nuclear target experiments due to excitation is enhanced by a factor A/Z.[9] Thus asymmetries of the order of 20% are to be expected, the signal being proportional to the real part of the Breit-Wigner amplitude[9]. Resonances at M^* = 1525 MeV (I = 1/2), 1688 MeV (I = 1/2), and 1920 MeV (I = 3/2) give photoabsorption $\sigma_{\gamma p}(\omega^*)$ cross sections of the order of 150 μb,[8] and thus give pair production asymmetries of the order of 1/4 that of the first resonance. In addition, information about the forward photon-neutron amplitude at the I = 1/2 resonances can be obtained from measurements of pair production on nuclear targets.

III. ISOBAR CALCULATION

In this section we present a more quantitative calculation of the Compton contribution to electron pair production in the region of the first nucleon resonance. We shall use a simple isobar model consistent with that used by Dufner and Tsai[6] in their recent analysis of electroproduction of the 3-3 resonance. As in Ref. 6, the γNN^* vertex will be assumed to be dominated by the Ml multipole; for real photons the E2 contribution is known to at most a few percent of Ml. In our calculations we shall ignore small background contributions from $B_1 \times B_2$, $B_1 \times C$, u channel resonances, vector mesons, and higher nucleon resonances, which are relatively slowly varying in the first resonance region. Unlike Eq. (9), the results will not be restricted to small δ.

The general matrix element of the electromagnetic current at the proton-N^* ($I = 3/2$, $J = 3/2$) vertex can be written as[6]

$$< P_f\lambda_f \mid J_\mu \mid P_i\lambda_i > = \mid e \mid \Psi^\nu(P_f,\lambda_f)\gamma_5\Big[C_3(\gamma\cdot q\, g_{\nu\mu} - q_\nu\gamma_\mu) + C_4(q\cdot P_f\, g_{\nu\mu} - q_\nu P_{f\mu})$$

$$+ C_5(q\cdot P_i\, g_{\nu\mu} - q_\nu P_{i\mu})\Big]\psi(P_i,\lambda_i) \qquad (10)$$

$$\equiv \mid e \mid \Psi^\nu(P_f,\lambda_f)\, V_{\nu\mu}(P_f,P_i)\,\psi(P_i,\lambda_i)$$

with $q = P_f - P_i$. The form factors C_3, C_4, and C_5 are functions only of q^2 when the proton and N^* are on their respective mass shells. The condition for pure M1 excitation at $q^2 = 0$ is[6]

$$C_4(0) = C_3(0)/M_{33}\ ,$$

$$C_5(0) = 0\ .$$

and where

$$M\cdot C_3(0) = 2.05 \pm 0.04$$

from the analysis of photoproduction experiments. The proton mass and the central value of the N^* mass distribution are denoted here by M and M_{33}. The propagator for the spin 3/2 resonance will be taken as

$$i\,\mathbb{P}_{\alpha\beta}(p) = -i\,\frac{\gamma\cdot p + M_{33}}{p^2 - M_{33}^2 + i M_{33}\Gamma(p^2)}\ \frac{1}{3M_{33}^2} \qquad (11)$$

$$\Big[3g_{\alpha\beta}M_{33}^2 - 4p_\alpha p_\beta - \gamma_\alpha\gamma_\beta M_{33}^2 + \gamma_\alpha\gamma\cdot p\, p_\beta + p_\alpha\gamma\cdot p\,\gamma_\beta\Big]$$

The contribution to the total pair production matrix element squared from the term $B_1 \times C^*$ (averaged and summed over spins and polarization) is[10]

$$2\,\mathrm{Re}\,\overline{\sum_{\substack{\text{spin,}\\ \text{pol}}} M_{C^*} M^{\dagger}_{B_1}} = 2\left(\frac{-e^6}{4q^2 k'^2}\right) T^{\nu\mu\tau} \times$$

$$\mathrm{Tr}\left\{\left(\frac{\gamma\cdot P' + M}{2M}\right) V_{\beta\nu}(P', P+k)\, P_{\beta\alpha}(P+k)\, V_{\alpha\mu}(P+k, P) \right. \qquad (12)$$

$$\left. \times \left(\frac{\gamma\cdot P + M}{2M}\right)\left[F_1(q^2)\gamma_\tau + \frac{\kappa}{4M} F_2(q^2)[\gamma\cdot q, \gamma_\tau]\right]\right\}$$

where the lepton trace is given by

(13)

$$T^{\nu\mu\tau} = \mathrm{Tr}\left[\left(\frac{\gamma\cdot p_- + m_e}{2m_e}\right)\gamma^\nu\left(\frac{\gamma\cdot p_+ + m_e}{2m_e}\right)\left\{\gamma^\mu \frac{\gamma\cdot k - \gamma\cdot p_+ + m_e}{-2k\cdot p_+}\gamma^\tau + \gamma^\tau \frac{\gamma\cdot p_- - \gamma\cdot k + m_e}{-2k\cdot p_-}\gamma^\mu\right\}\right]$$

The momenta are defined in Fig. 1a.

The contribution of Eq. (12) to the cross section can be written in terms of five invariants. The complete answer is extremely long and we shall only give results appropriate to small angle experiments.

Let us now consider electron pair production on hydrogen. When both leptons are detected at angles $\theta_\pm \leq 20^\circ$, it is sufficient to expand the interference term in the cross section to second order in the lepton production angles θ_+ and θ_-. This small angle approximation is adequate as well for single lepton detection experiments since the undetected lepton tends to choose an angle which minimizes the propagators. Electron mass terms can be safely ignored as well, since no $m_e^2/(k\cdot p_\pm)^2$ terms arise in the interference term. At small angles only the convection part of the nucleon current in the B_1

amplitude contributes to the interference term. The small angle expansion of Eq. (12) is $(q^2 = -\vec{q}^{\,2})$

$$2\mathrm{Re}\sum_{\substack{\text{spins,}\\ \text{pol}}} M_{C^*} M^{\dagger}_{P_1} = (X_1 - X_2)\,\frac{s - M_{33}^2}{(s - M_{33}^2)^2 - M_{33}^2\Gamma^2}\,\frac{C_3^2 M}{3M_{33}^3 m_e^2}\,\frac{8}{q^2 (p_1 + p_2)^2} \tag{14}$$

where

$$\begin{aligned} X_1 = \frac{1}{2k\cdot p_1}\Bigg\{ & \left[M^3 + 2M M_{33}^2 + 3 M_{33}^3\right] \\ & \Big[q^2(E_1^3 + E_1^2 E_2 + E_1 E_2^2 + E_2^3) + \theta_1^2 (E_1^5 + 3E_1^4 E_2 + 3 E_1^3 E_2^2 + 3 E_1^2 E_2^3 + 2 E_1 E_2^4) \\ & \qquad + \theta_2^2 (E_1^3 E_2^2 + E_1^2 E_2^3 + E_1 E_2^4 + E_2^5)\Big] \\ & + 2M^2 \Big[q^2 (E_1^4 + 2 E_1^3 E_2 + 2 E_1^2 E_2^2 + 2 E_1 E_2^3 + E_2^4) \\ & + \theta_1^2 (E_1^6 + 4 E_1^5 E_2 + 6 E_1^4 E_2^2 + 6 E_1^3 E_2^3 + 5 E_1^2 E_2^4 + 2 E_1 E_2^5) \\ & + \theta_2^2 (E_1^4 E_2^2 + 2 E_1^3 E_2^3 + 2 E_1^2 E_2^4 + 2 E_1 E_2^5 + E_2^6)\Big]\Bigg\} \end{aligned} \tag{15}$$

and

$$X_2 = X_1 (p_1^{\mu} \longleftrightarrow p_2^{\mu}) .$$

The cross section including Bethe-Heitler and N^* interference contributions is

$$d\sigma = d\sigma_{B_1}\left(1 + \frac{d\sigma_{int}}{d\sigma_{B_1}}\right)$$

where

$$\frac{d\sigma_{int}}{d\sigma_{B_l}} = \frac{(X_1 - X_2)}{\lambda_{ll}} \frac{s - M_{33}^2}{(s - M_{33}^2)^2 + \Gamma^2 M_{33}^2} \frac{1}{(p_1 + p_2)^2} \frac{1}{q^2} \frac{32\, C_3^2\, M}{3\, M_{33}^3}$$

$$\equiv K \frac{s - M_{33}^2}{(s - M_{33}^2)^2 + \Gamma^2 M_{33}^2} C_3^2 \qquad (16)$$

and the Bethe-Heitler contribution λ_{ll} is defined in Eq. (4). The interference contribution changes sign when the electron and positron momenta are interchanged.

In Figs. 2 and 3 we show the predicted asymmetry

$$\epsilon(\delta, k) = \frac{N_+(\delta) - N_-(\delta)}{N_+(\delta) + N_-(\delta)} \cong \frac{d\sigma_{int}}{d\sigma_{B_l}} \left(E_- = \frac{k+\delta}{2},\ E_+ = \frac{k-\delta}{2}\right) \qquad (17)$$

due to the first s-channel nucleon resonance for coincidence measurements of near-symmetric electron-positron pairs[11]. Here $N_-(\delta)$ [$N_+(\delta)$] is the production rate when the electron and positron are detected symmetrically but the electron [positron] has δ less momentum than the other lepton. Since the asymmetry is generally less than 20% the neglect of the $C^* \times C^*$ contribution is justified.

In each figure, two curves are shown for two choices of the form of s-dependence of the resonance width[6]:

$$\Gamma_a(s) = 120\ (p_\pi^*/p_R^*)^3\ \text{MeV}$$

$$\Gamma_b(s) = 127.5\ (0.85\, p_\pi^*/m_\pi)^3/(1 + (0.85\, p_\pi^*/m_\pi)^2)\ \text{MeV} \qquad (18)$$

where p_π^* is the pion momentum in the rest frame of the N^*;

$$[p_\pi^*(s)]^2 = [(s - M^2 + m_\pi^2)/2\sqrt{s}]^2 - m_\pi^2, \quad \text{and} \quad p_R^* = p_\pi^*(M_{33}^2).$$

Note that we have not assumed any energy dependence of the vertex parameter C_3. Although the proposed experiments are difficult, an experimental determination of the correct form of $\Gamma(s)$ would seem to be feasible and the results should be of considerable theoretical interest. The direct determination of the real part of the resonant amplitude would be obtained from the measurement of the quantity

$$\epsilon(\delta, k)\, K^{-1}$$

where K is the known kinematic factor defined in Eq. (16).

IV. COMPTON MEASUREMENTS ON NUCLEAR TARGETS

Pair production and bremsstrahlung experiments are more easily performed on nuclear targets such as carbon rather than hydrogen. Fortunately, considerable information on the nucleon Compton amplitudes can still be obtained from the asymmetric experiments[12].

For photon energies greatly exceeding the binding energy, impulse approximation is justified for the nucleon pole contribution f_C to the nuclear Compton amplitude. For Dirac nucleons (an adequate approximation for small angle Compton scattering) the corresponding nuclear amplitude is

$$F_C = \int \prod_{i=1}^{A} d^3x_i \, \phi_f^\dagger(\vec{x}_1 \ldots \vec{x}_A) \sum_{i=1}^{Z} f_C^{(i)} e^{-i\vec{q}\cdot\vec{x}_1} \phi_i(\vec{x}_1 \ldots \vec{x}_A) = ZG_A(q^2) f_C \qquad (19)$$

where $G_A(q^2)$ is the nuclear charge form factor. This has the same functional dependence on q^2 as the Bethe-Heitler amplitudes. The results for $\epsilon_{pole}(\delta)$ are thus independent of the nuclear form factor and are identical to the proton target result.

For the case of the isobar Compton amplitudes, the impulse approximation, (i.e., treating each nucleon independently), is not adequate since the nucleon resonance is apt to be absorbed in the nuclear medium. We can estimate that the mean free path for an N^* in a nucleus to be $\mu \approx 2F$, corresponding to a total $N\text{-}N^*$ cross section of ≈ 40 mb at $|\vec{p}| = k \approx 350$ MeV. This leads to decay by absorption in a time

$$\tau_{abs} = \frac{\mu}{\text{Velocity}} = \frac{\mu}{k/M_{33}} \approx \frac{1}{30 \text{ MeV}}$$

compared to

$$\tau_{decay} = \frac{1}{\Gamma} = \frac{1}{120 \text{ MeV}} \, .$$

Thus the effective width is increased in an energy-dependent manner:

$$\Gamma \Rightarrow \Gamma + \frac{k}{M_{33}} \frac{1}{\mu} \, , \qquad (20)$$

roughly a 25% correction at resonance. The effect of absorption can be summarized by using the form

$$\frac{1}{s - M_{33}^2 + iM_{33}\Gamma - V}$$

for the resonant amplitude in the nuclear medium, where $V = -ik/\mu$ is an absorptive optical potential. This collision broadening effect would also be observable in nuclear Compton and pion-nucleus scattering in the resonance region.

The impulse approximation is adequate for the isobar Compton amplitudes when the effective increased width form of Γ is used[13]. Since protons and neutrons contribute equally for $I = 3/2$ resonances, the asymmetry ϵ is increased by a factor A/Z in pair production experiments. If the proton and neutron distributions are identical, then, in addition, the contribution to ϵ is independent of the nuclear form factor.

V. CONCLUSION

The results given in the previous sections indicate that the fractional asymmetry due to the isobar resonances is sufficiently large and sufficiently sensitive to width corrections for a practical experiment. Although experiments on hydrogen would be the most useful, experiments on low Z nuclear targets can also give important information on the real part of the Compton amplitude. The collision broadening complication discussed in Section IV can be resolved by measuring photon-nucleus or pion-nucleus scattering. In fact, a measurement of the increase of the isobar resonance width in nuclear matter is interesting in its own right since this yields a determination of the $N\text{-}N^*$ total cross section.

In fact, several asymmetric electron pair production measurements on carbon have already been performed.[4,5,14] Of these, the only experiment sensitive to the effect of the first nucleon resonance was the single lepton rate measurements of Simonds[5]. In the "single arm" experiments the detected lepton is required to have nearly the maximum bremsstrahlung energy in order to define the photon energy and avoid background from π^o production. The experimental results were sufficiently sensitive to show a positive fractional symmetry ϵ for k above 350 MeV. This is consistent with Fig. 2.

It is expected, however, that the most detailed determination of the real part of the virtual Compton amplitude, i.e., checks of isobar resonance shape, the dispersion relation Eq. (1), and the γNN^* vertex form factor, will come from coincidence measurement of asymmetric electron pairs or the electron-positron bremsstrahlung ratio.

ACKNOWLEDGMENTS

We would like to thank Dr. R. Simonds for stimulating our interest in the asymmetric pair production experiments. We also acknowledge useful discussions with Professor T. A. Griffy, Dr. J. Pumplin, Dr. A. Krass, Dr. Y. S. Tsai and Professor J. Bjorken.

REFERENCES

1. Ambiguities in the analysis of proton Compton scattering are discussed, for example, by S. Minami, Nuovo Cimento 47, 64 (1967).
2. S. Brodsky and J. Gillespie, Phys. Rev. 173, 1011 (1968).
3. Recent results are summarized by S. C. C. Ting, Rapporteur's Summary, Proceedings of the XIV International Conference on High Energy Physics, Vienna, 1968, p. 43.
4. J. G. Asbury et al., Phys. Letters 25B, 565 (1967). The effects of the Compton amplitude on such experiments was first discussed by S. D. Drell, Phys. Rev. Letters 13, 257 (1964).
5. A pioneering exploratory experiment of this type has been performed by R. M. Simonds (Stanford University Thesis, 1968, unpublished). His work has provided much of the motivation for this work.
6. A. J. Dufner and Y. S. Tsai, Phys. Rev. 168, 1801 (1968). Experimental references are W. Bartel et al., DESY reports 68/42 and 68/53. H. Lynch et al., Phys. Rev. 164, 1635 (1967) and references therein.
7. J. D. Bjorken, S. D. Drell, and S. C. Frautschi, Phys. Rev. 112, 1409 (1958). Their expression for λ_{12} must be multiplied by $-1/M^2$.
8. For a recent compilation the inelastic electron scattering data, see W. K. H. Panofsky, Proceedings of the XIV International Conference on High Energy Physics, Vienna, 1968, p. 23.
9. Some broadening of the width function Γ due to nuclear effects is expected, however. See Section IV.
10. An alternative approach to this calculation is to follow the method of Berg and Lindner, Phys. Rev. 112, 2072 (1958). The pair production and

bremsstrahlung cross sections are calculated for the Bethe-Heitler graphs and for the general Compton amplitude using the 12 independent virtual Compton amplitudes. The contribution of the resonance amplitude is then obtained by calculating the resonance contribution to the 12 Berg-Lindner amplitudes. We have verified their results for the interference term (Eq. 2.6), using the algebraic computer program REDUCE developed by one of the authors (A. C. H.). We have also verified the calculations of the projections $f_1 \ldots f_{12}$ for the proton Born contributions (Eq. 4.4), with the exception of f_8 which should be

$$\frac{F_1(2\nu_2\nu_3 - \nu_2^2\mu) + \mu F_2(\nu_2^2 + 2\nu_2\nu_3 + \nu_1^2\nu_3\mu - \nu_2^2\nu_3\mu)}{2(\nu_2 + \nu_3)(\nu_1^2 - \nu_2^2)} .$$

This error has also been noted by M. Greco, A. Tenore and A. Verganelakis, Phys. Letters 27B, 317 (1968) and (unpublished). The latter authors give the projections $f_1 \ldots f_{12}$ for the 3-3 resonance assuming only the C_3 interaction which, however, does not correspond to M1 excitation.

11. The application to single-lepton detection experiments is discussed in Section V.

12. In principle, one could use asymmetric pair production to test the Kramers-Kronig relation analogous to (1) for forward photon-nucleus Compton scattering, with $A(\omega = 0, 0^\circ) = -Z^2\alpha/M_A$. The relevant photon energy region for the pair production experiments would, however, be k ~ binding energy.

13. In principle, there are also contributing multinucleon amplitudes with strong energy dependence at $s \sim M_{33}^2$, such as the amplitude representing

the two nucleon process,

$$\gamma + p_1 + p_2 \rightarrow N^* + p_2 \rightarrow p_1' + \pi + p_2 \rightarrow p_1' + N^* \rightarrow \gamma' + p_1' + p_2'.$$

However such contributions are considerably suppressed by (1) the small overlap with the abnormal parity nucleon intermediate state, and (2) the large absorption suffered by the intermediate state pion and nucleon, greatly increasing the energy denominator. Shadowing of the interior nucleus due to coherent ρ photoproduction is not important for $k \lesssim 2$ BeV. See, e.g., S. Brodsky and J. Pumplin, Phys. Rev. (to be published).

14. B. Richter, Phys. Rev. Letters 1, 203 (1958). V. W. Hughes et al., Proceedings of the International Symposium on Electron and Photon Interactions at High Energies (Hamburg, 1965), p. 361. K. J. Cohen et al., Phys. Rev. 173, 1315 (1968).

FIGURE CAPTIONS

Figure 1 Feynman diagrams for electron pair production. Figures (a) through (e) give the Bethe-Heitler amplitude through second order in the electromagnetic interaction with the nucleus. Diagram (f) represents the virtual Compton contribution to pair production and includes contributions from the nuclear pole terms, nucleon and nuclear excitations, and neutral vector meson production. In this paper we are primarily concerned with the kinematic regions where the Compton contribution to pair production is dominated by isobar excitation.

Figure 2 Electron-positron asymmetry in pair production of protons due to the $N^*_{3/2}(1236)$ Compton interference contribution versus photon laboratory energy as given by Eqs. (15)-(17). The two curves correspond to choices for the energy dependence of the resonance width given in Eq. (18). Contributions to ϵ due to the nucleon pole diagrams, other resonances, and second Born corrections are not included.

Figure 3 Electron-positron asymmetry in pair production on protons due to the $N^*_{3/2}(1236)$ Compton interference contribution versus the lepton energy difference as given by Eqs. (15)-(17). Curves are shown for the laboratory photon energy below and above the resonance energy and for two choices of energy dependence of the isobar width (see Eq. (18)). Contributions to ϵ due to the nucleon pole diagrams, other resonances, and second Born corrections are not included.

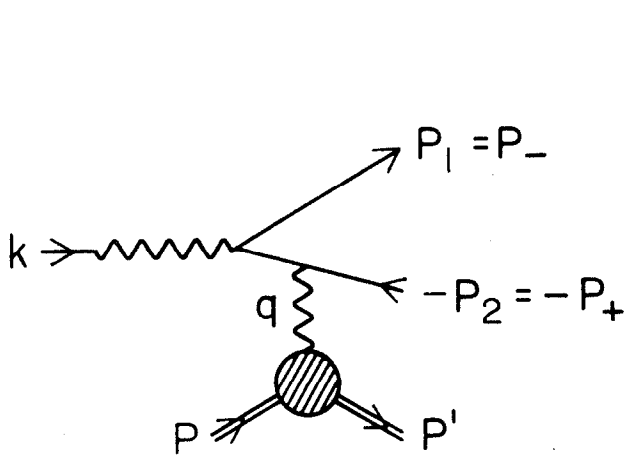

(a)

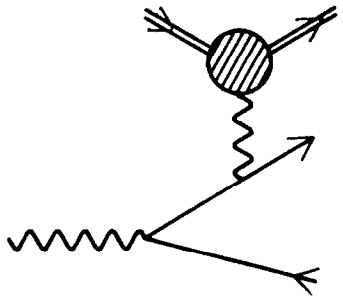

(b)

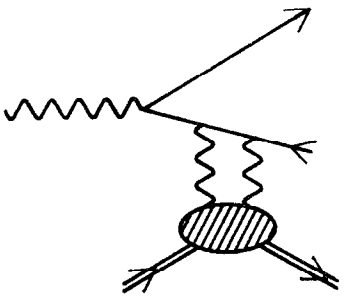

(c)

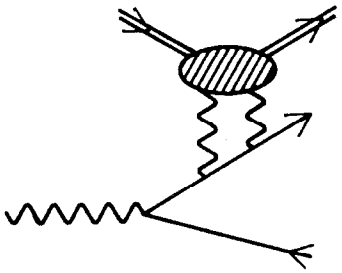

(d)

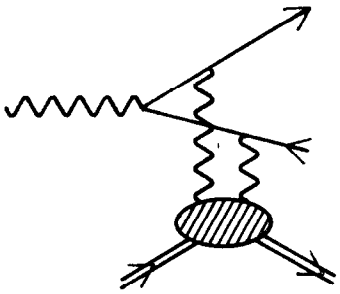

(e)

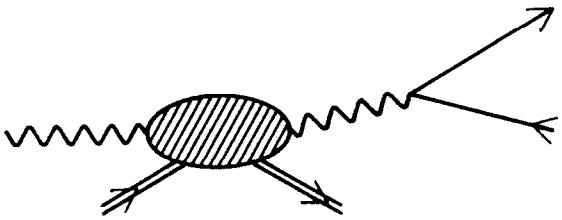

(f)

988A1

Fig. 1

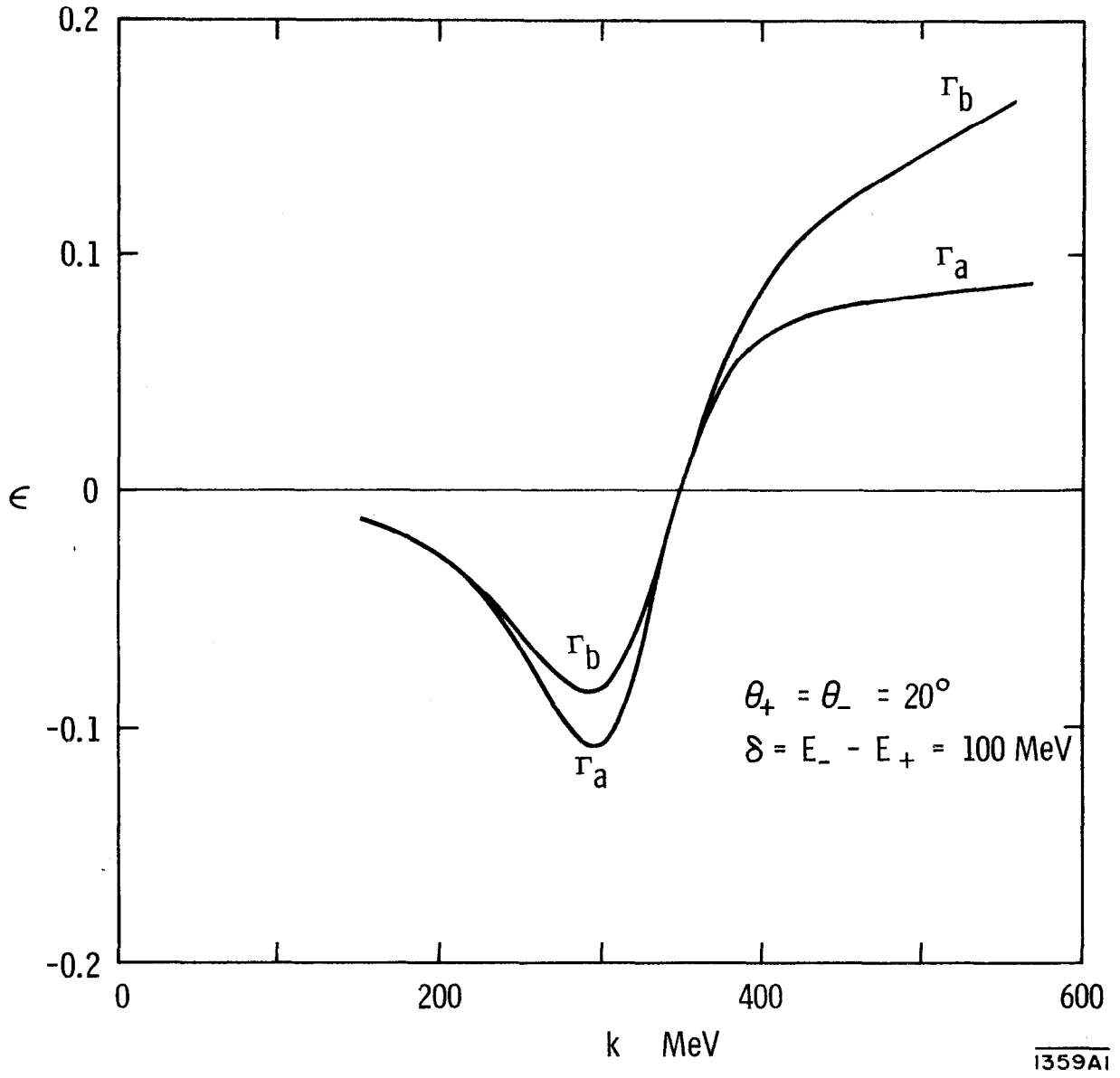
0.2
0.1
0
-0.1
-0.2
ϵ
0
200
400
600
k MeV
r_b
r_a
r_b
r_a
$\theta_+ = \theta_- = 20°$
$\delta = E_- - E_+ = 100$ MeV
1359A1

Fig. 2

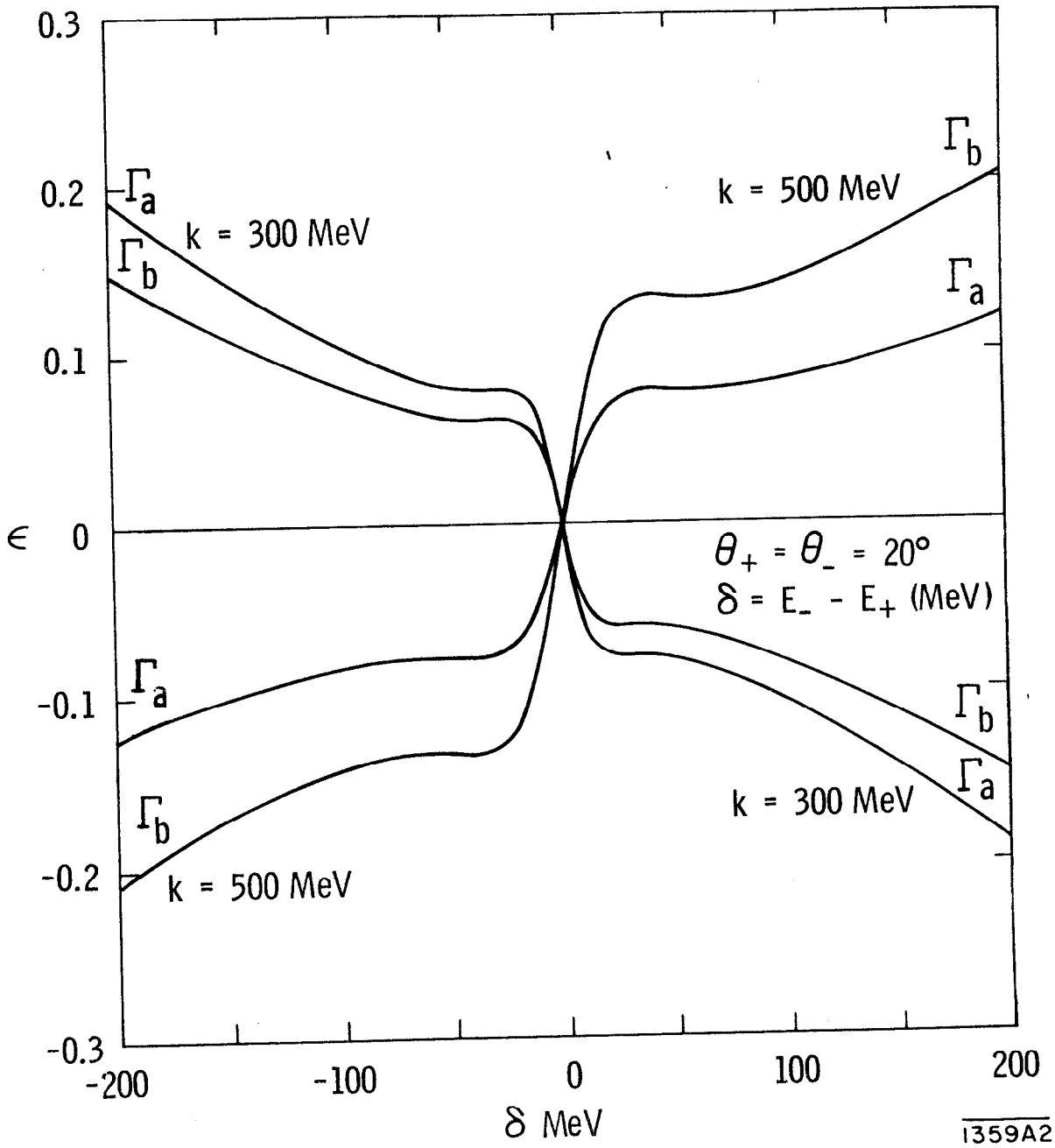
0.3
0.2
0.1
0
-0.1
-0.2
-0.3
ϵ
-200
-100
0
100
200
δ MeV
Γa
Γb
k = 300 MeV
k = 500 MeV
Γb
Γa
θ+ = θ− = 20°
δ = E− - E+ (MeV)
Γa
Γb
k = 300 MeV
Γb
Γa
k = 500 MeV
1359A2

Fig. 3